

Anchor-Based Spatial-Temporal Attention Convolutional Networks for Dynamic 3D Point Cloud Sequences

Guangming Wang, Hanwen Liu, Muyao Chen, Yehui Yang, Zhe Liu, and Hesheng Wang

Abstract—Recently, learning based methods for the robot perception from the image or video have much developed, but deep learning methods for dynamic 3D point cloud sequences are underexplored. With the widespread application of 3D sensors such as LiDAR and depth camera, efficient and accurate perception of the 3D environment from 3D sequence data is pivotal to autonomous driving and service robots. An Anchor-based Spatial-Temporal Attention Convolution operation (ASTACConv) is proposed in this paper to process dynamic 3D point cloud sequences. The proposed convolution operation builds a regular receptive field around each point by setting several virtual anchors around each point. The features of neighborhood points are firstly aggregated to each anchor based on spatial-temporal attention mechanism. Then, anchor-based sparse 3D convolution is adopted to aggregate the features of these anchors to the core points. The proposed method makes better use of the structured information within the local region, and learn spatial-temporal embedding features from dynamic 3D point cloud sequences. Then Anchor-based Spatial-Temporal Attention Convolutional Neural Networks (ASTACNNs) are proposed for classification and segmentation tasks and are evaluated on action recognition and semantic segmentation tasks. The experimental results on MSRAction3D and Synthia datasets demonstrate that the higher accuracy can be achieved than the previous state-of-the-art method by our novel strategy of multi-frame fusion.

Index Terms—Point clouds, 3D deep learning, spatial-temporal embedding, action recognition, semantic segmentation.

I. INTRODUCTION

The perception of the 3D environment is important for the Simultaneous Localization And Mapping (SLAM), navigation, and decision making of autonomous driving. Some mainstream sensors, such as depth cameras and LiDAR, can directly get the dynamic 3D point cloud sequences of the environment, which contain abundant spatial-temporal information. Thus, studying effective feature extraction methods for the 3D point clouds has been the focus of the community in recent years. Latest

This work was supported in part by the Natural Science Foundation of China under Grant U1613218, 61722309, and U1913204, in part by Beijing Advanced Innovation Center for Intelligent Robots and Systems under Grant 2019IRS01. Corresponding Author: Hesheng Wang (e-mail: wanghesheng@sjtu.edu.cn).

G. Wang, Yehui Yang, and H. Wang are with the Department of Automation, Institute of Medical Robotics, Key Laboratory of System Control and Information Processing of Ministry of Education, Key Laboratory of Marine Intelligent Equipment, and System of Ministry of Education, Shanghai Jiao Tong University, Shanghai 200240, China. H. Wang is with Beijing Advanced Innovation Center for Intelligent Robots and Systems, Beijing Institute of Technology, China. H. Liu and M. Chen are with the Department of Computer Science and Engineering, Shanghai Jiao Tong University, Shanghai 200240, China. Z. Liu is with the Department of Computer Science and Technology, University of Cambridge.

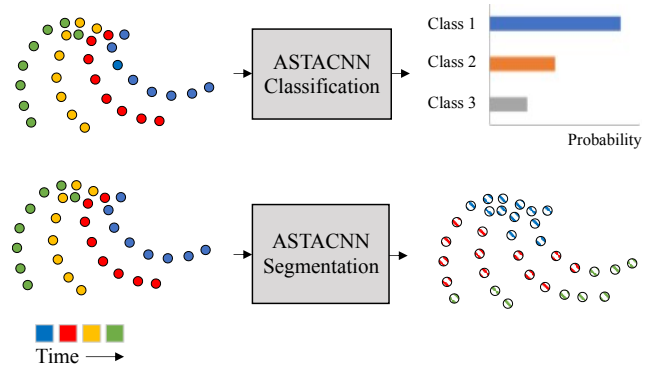


Figure 1. Our Anchor-based Spatial-Temporal Attention Convolutional Neural Networks (ASTACNNs) can directly learn spatial-temporal information from dynamic 3D point cloud sequences using discrete convolution kernel in an end-to-end fashion. This paper demonstrates the performance in classification and segmentation tasks.

works [1]–[4] show the potential of directly consuming points, and they do not need to convert the point clouds into other forms, such as voxel form [5]–[8]. Many works have explored the learning of single point cloud on 3D object retrieval [9]–[11], classification [1], [2], and segmentation [12]–[14]. There are a few pieces of research on the learning of multi-frame point cloud, and there remain some challenges.

Recently, some methods [15], [16] are proposed to use the end-to-end deep learning network to process the point cloud sequences, but these methods convert point clouds into grid representations. The grid quantization error is inevitable. Moreover, the extra conversion will cause inefficient processing performance. It is not conducive to run in real-time situations. Latest work, MeteorNet [4] handles the point cloud sequences directly by adding time encoding with the position and feature encoding in PointNet++ [2]. In [4], the chained-flow grouping relies on the accuracy of scene flow estimation, and the direct grouping uses varying radius for different frames. It is still a challenge to extract structured features from unordered point cloud sequences without converting the data forms. In this paper, we focus on a novel sparse 3D convolution method for dynamic 3D point cloud sequences based on direct grouping, not relying on extra scene flow estimation [4]. Inspired by the recent interpolated convolution methods [12], [14] on a single frame of 3D point clouds, we design an anchor-based spatial-temporal attention convolution to deal with dynamic 3D point cloud sequences. The results demonstrate that our structured spatial-temporal attention con-

volution design benefits a lot to the tasks for 3D point cloud sequences.

In this paper, an anchor-based spatial-temporal attention convolution (ASTAConv) is proposed, which has a structural 3D convolution kernel applied on each real point location and extracts structural features by the designed 3D convolution kernel from the sparse and irregular point cloud sequence data. Multiple virtual anchors are established around each real point with the learnable convolution weights. The structural features from 3D points around these anchors are firstly learned and embedded into these virtual anchors by a spatial-temporal attention encoding. The proposed spatial-temporal encoding method encodes the original features of spatial coordinates, timestamps, and point features to the structured features in anchors. Then, a predefined 3D convolution kernel based on the structure of anchors is adopted to extract structural features from these anchors to obtain the final features of each real point, the kernel center of the anchor-based convolution kernel. The first spatial-temporal attention encoding structurally organizes the original unordered and irregular data in a learnable fashion. Then, the anchor-based 3D convolution method makes the 3D feature extraction. The proposed method contributes to the 3D feature extraction from dynamic 3D point cloud sequences in a full learnable fashion, without the interpolation calculation [12], [14].

Based on the ASTAConv, we propose Anchor-based Spatial-Temporal Attention Convolutional Neural Networks (ASTACNNs), including the classification network and segmentation network. As visualized in Fig. 1, the classification network can obtain the probabilities that the point cloud sequences belong to each category. The segmentation network can output the probabilities that each point in point cloud sequences belongs to each category, and the category with the highest probability of each point serves as the segmentation category for each point. The contributions are as follows:

- A novel Anchor-based Spatial-Temporal Attention Convolution operation (ASTAConv) is proposed in this paper. By introducing a discrete 3D convolution kernel on multiple virtual structured anchors after 1×1 convolution, the 3D features can be structurally extracted.
- To gather irregular and unordered points to the virtual anchors, the spatial-temporal attention encoding is proposed to learn to weight the points around each anchor. The spatial-temporal attention encoding considers the euclidean space, feature space, and time space. The soft weighted method is used to replace the classical max pooling.
- We further propose Anchor-based Spatial-Temporal Attention Convolutional Neural Networks (ASTACNNs) for the classification and segmentation tasks. Experiments on MSRAAction3D dataset [17] and Synthia dataset [18] show that the proposed networks achieves superior performance compared with the state-of-the-art methods. The ablation studies demonstrate the effectiveness of each design.

The rest of this article is organized as follows. Section II summarizes recent works related to this paper. Section III describes the proposed anchor-based spatial-temporal attention

model. Section IV shows the experiment results and visualization on Synthia dataset [18]. Finally, the conclusion is drawn in Section V.

II. RELATED WORK

A. Deep Learning on the Single Frame of Point Clouds

PointNet [1] is a pioneering work in applying deep learning to consume point clouds directly. The primary approach is to construct a symmetric function, where it uses shared Multi-layer Perceptrons (MLP) to aggregate neighborhood information of each point and then uses an element-wise max pooling to extract local features. The continuation work PointNet++ [2] extracted and aggregated neighborhood features hierarchically in the Euclidean space around each point.

Recent works made some innovations in the design of the convolution kernel. SPLATNet [19] used the high-dimension mesh to carry features of input points and then extracted features by adopting the bilateral convolution. SpiderCNN [20] proposed to apply different weights to each convolution kernel for each neighbor. Komarichev et al. [21] utilized annular convolution for point clouds before regular convolution operations by considering orbicular structures and directions. Method of Lei et al. [22] used spherical convolution kernel to separate the space and extracted features. Zhao et al. [23] applied the dense connection between every two points in the local neighborhood by Adaptive Feature Adjustment (AFA) to represent better than DGCNN [24]. ShellNet [25] used the max pooling for overall points in each concentric spherical shell and was applied to semantic segmentation and object classification tasks. Different from these works, ours focuses on shared discrete convolution on the feature extraction of each point from 3D point clouds, just like the successful convolutional neural networks (CNNs) on 2D images.

KPCConv [3] also learned the weights of structural positions in space. However, KPCConv [3] sampled the 3D point clouds for the network input and used designed linear correlation in the convolution. While ours uses the anchor-based 3D convolution (implemented by $1 \times m$ convolution kernel) to extract discrete local features, which learns geometry explicitly. Mao et al. [12] used an interpolated convolution method for 3D point clouds, which is consistent with the traditional discrete convolution method. However, the interpolation function is artificially designed, which can not adjust to the change of local point clouds. While our method can retain the superiority of local adaptation by the spatial-temporal attention encoding. Besides, learning-based local encoding makes ours can handle dynamic 3D point cloud sequences.

Some recent works [13], [26], [27] also used convolution twice, but they only used 1×1 convolution kernel. In this paper, different sizes of convolution kernels are introduced: 1×1 and $1 \times m$. The first 1×1 convolution organizes and encodes spatial-temporal information from unordered and irregular point clouds. Then, the structured information is extracted by the second $1 \times m$ convolution.

B. Deep Learning on the Dynamic 3D Point Cloud Sequences

In MinkowskiNet [15], 3D point cloud sequences are converted into 4D occupancy grids to deal with time se-

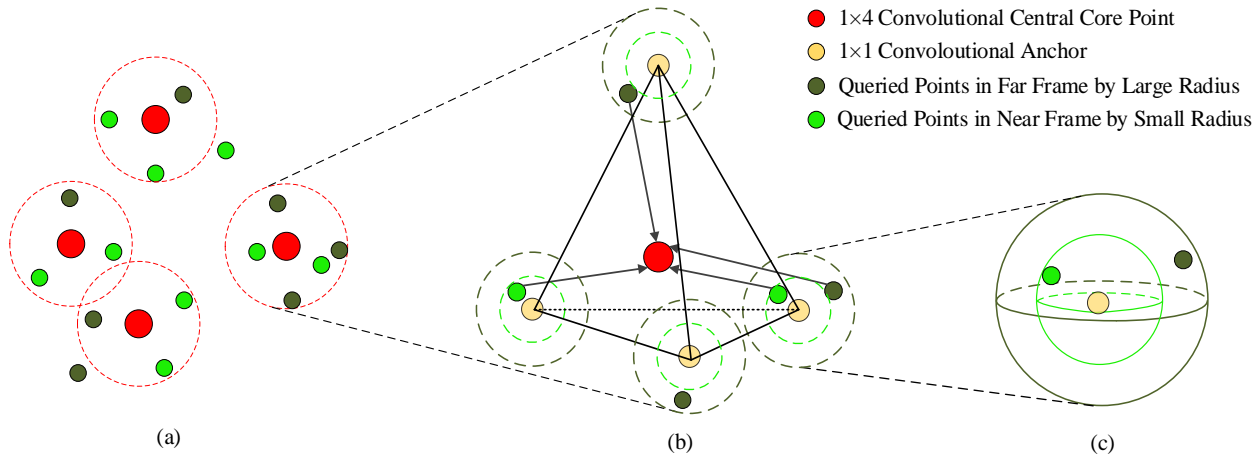


Figure 2. The overview of the proposed anchor-based spatial-temporal convolutional operation for dynamic 3D point cloud sequences. (a) Input 3D point clouds from multiple frames. Red points represent the selected core points for the 1×4 convolution. Light green points and dark green points respectively represent points of the near frame and far frame from the current frame. (b) The details of an anchor-based convolutional operation. Light yellow points represent the 4 anchors constructed as a regular tetrahedron form. Anchors are virtual points occupying the spatial location, and at these coordinates, there may not be real points from the 3D point cloud sequences. (c) Querying neighborhood points around an anchor from multiple frames. To gather surrounding points from multiple frames, different radii are considered for the ball querying. The detailed formulation of choosing radii is shown in Section III-B. Spatial-temporal attention encoding is used to obtain the features of anchors. 1×4 convolution is then adopted to extract structured features from 4 anchors.

quences directly, and then the sparse 4D convolution is used. HPLFlowNet [28], inspired by bilateral convolution layers [29], [30], introduced DownBCL, UpBCL, and CorrBCL operations, which transferred point clouds to structured information and used the convolution, but the manual interpolation is used for data preprocessing. Different from converting raw 3D point clouds to grids or voxels, the proposed method can directly consume dynamic 3D point cloud sequences without losing information in the data preprocessing.

FlowNet3D [31], based on PointNet++ [2], used flow embedding layer to associate two point clouds, and generated scene flows from the flow embedding features by the flow refinement. [26] and [27] used the point cost volume to associate two point clouds. The point cost volume is also based on shared MLP, implemented by 1×1 convolution. These methods only for two point clouds to find local correspondence. MeteorNet [4] is one leading method of deep learning methods for dynamic 3D point cloud sequences. The structure of MeteorNet [4] is inherited from PointNet [1] and used shared MLP, while our network uses a novel anchor-based spatial-temporal attention convolution operation. Experiments show that the proposed novel convolution operation greatly enhances the performance of networks.

III. ANCHOR-BASED SPATIAL-TEMPORAL ATTENTION CONVOLUTIONAL NEURAL NETWORK

A novel Anchor-based Spatial-Temporal Attention Convolution operation (ASTAConv) is proposed to gather information from multi-frame point clouds structurally. Then this operation is used to build classification and segmentation networks. The anchor-based convolution kernel is introduced in Section III-A. The features of anchors are obtained through the spatial-temporal attention encoding in Section III-B. The proposed Anchor-based Spatial-Temporal Attention Convolutional Neural Networks (ASTACNNs) are introduced in Section III-C.

A. Anchor-Based 3D Convolution Kernel

The previous method [4] based on 3D point clouds does not make full use of the structural features of point cloud sequences. Therefore, the anchor-based convolution model is proposed in this paper. The neighborhood spatial-temporal features are first embedded to anchors, and then the proposed anchor-based convolution kernel is applied to gather features of anchors. The anchors are expanded and connected with each convolutional central core point as shown in Fig. 2(b). The novel convolution kernel gathers the neighborhood information from raw unordered and irregular point cloud sequences in a structural fashion but avoids using the indeterminate manual interpolation [26], [27].

The overview of the proposed anchor-based spatial-temporal convolution model is shown in Fig. 2. In this model, the real points $P = \{p_i = \{x_i, f_i, t_i\} | i = 1, 2, \dots, N\}$ serve as central core points of the anchor-based convolution. $x_i \in \mathbb{R}^3$ represent the 3D coordinates, $f_i \in \mathbb{R}^d$ represent the raw feature, and $t_i \in \mathbb{N}$ represent the timestamp (order of the frame) of the point p_i . Considering the symmetry of the spatial structure, a regular tetrahedron is used to generate 4 anchors $A_i = \{a_i^j = \{x_i^j, t_i^j\} | j = 1, 2, 3, 4\}$ from each central core point p_i . The 4 anchors are located at the 4 vertices of the regular tetrahedron:

$$\begin{bmatrix} x_i^1 \\ x_i^2 \\ x_i^3 \\ x_i^4 \end{bmatrix} = \begin{bmatrix} x_i \\ x_i \\ x_i \\ x_i \end{bmatrix} + \Delta X \cdot S, \quad (1)$$

$$t_i^j = t_i, \quad (2)$$

where x_i^j ($j = 1, 2, 3, 4$) and t_i^j are respectively the coordinates and the timestamp of the anchor related with the core point p_i . $\Delta X \in \mathbb{R}$ is a scalar and represents the size of the regular tetrahedron, which decides the distance between the central

point and anchors. S is a hyperparameter set according to the defined anchor forms. For the regular tetrahedron in this paper, S is defined as follows:

$$S = \begin{bmatrix} \frac{\sqrt{2}}{3}, & -\frac{\sqrt{6}}{3}, & -\frac{1}{3} \\ \frac{\sqrt{2}}{3}, & \frac{\sqrt{6}}{3}, & -\frac{1}{3} \\ -\frac{2\sqrt{2}}{3}, & 0, & -\frac{1}{3} \\ 0, & 0, & 1 \end{bmatrix}. \quad (3)$$

Each line in S defines the relative position of one anchor to the central point. Note that anchors are virtual coordinates together with virtual timestamps in the 3D space around the central core points, and real points are not required to appear at these locations.

To this step, the coordinates and the timestamps of anchors have been obtained. With these anchors as the centers of balls, neighborhood features from different frames are gathered by ball query [2]. Different from previous work [4], which directly gathers points around the core points, the proposed method gathers points based on anchors. In this way, the proposed method can make use of the structured 3D convolution on dynamic 3D point cloud sequences. The successful experience of discrete convolution on images can be applied to point clouds without the need for interpolation [12].

As mentioned before, the feature extraction for central core points can be divided into two steps. The details of the first step to gather features of the neighborhood points to anchors are described in Section III-B. After the first step, the features of anchors are obtained, represented by Γ_i^j ($j = 1, 2, 3, 4$). With these features, the features of central points can be extracted through the proposed anchor-based convolution. In this convolution, the convolution kernel size 1×4 is corresponding to the number of anchors around each central core point in 3D space.

$$O_i = \sigma\left(\sum_{j=1}^4 \omega_{ij} \Gamma_i^j + b_j\right), \quad (4)$$

where O_i represents the learned feature of the core point p_i from features of anchors by using 3D convolution. ω_{ij} and b_j are the convolution kernel parameters. σ is the activation function, which represents the Rectified Linear Unit (ReLU) here. That is, a self-defined 3D convolution is implemented by customizing the positions of convolution kernel parameters ω_{ij} ($j = 1, 2, 3, 4$). Other 3D forms of the convolution kernel can also be defined by the anchor-based approach. The regular tetrahedron based 3D convolution kernel is adopted here because this is the 3D symmetric convolution kernel with the least learning parameters.

Different from the traditional $n \times n \times n$ 3D convolution, the positions of learning parameters of our 3D convolution is defined by the anchors. As the anchors are located at the 4 vertices of the regular tetrahedrons, so the 1×4 convolution is required. Compared with the traditional 1×1 convolution method (Shared MLP) usually used in point clouds, a larger convolution kernel can explicitly learn the spatial structure from 3D point clouds. At the same time, the proposed network can directly consume multi-frame dynamic 3D point clouds as follows.

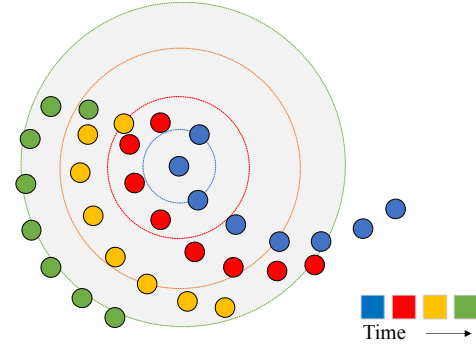


Figure 3. Radius increases with the time frame interval. The radius for the farther frame is larger in order to receive information that matches the current frame.

B. Spatial-Temporal Attention Encoding

The anchor-based convolution in Section III-A excavates the structural information of point clouds by anchors. In this part, the method of capturing spatial-temporal information for anchors is presented. The overview of this encoding module together with the anchor-based model is as shown in Fig. 4.

In the proposed method, relative coordinates and timestamps of neighborhood points to anchors will be embedded to each anchor, which strengthens local spatial-temporal awareness. This module also gathers raw features at the same time. The motivation for the attention encoding is that the point clouds from different frames have different influences on the classification or segmentation. Usually, points with closer timestamps have bigger influences. At the same time, max pooling is given up for retaining more information. In total, this method contains the following steps:

1) *Querying Neighborhood Points around Anchors from Multiple Frames*: To sufficiently use the information from multiple frames, a method to select neighborhood points of different frames is needed. Considering the movement of objects, a natural idea is that as the time interval increases, a broader area is searched for the points. That is, different radii are adopted to search for the points from different frames as shown in Fig. 3. A larger radius is adopted for far frames when gathering points so that there is a greater probability of receiving features in different frames that are associated with anchors.

These radii are applied to select points around an anchor from different frames. The radii are regarded as the maximum Euclidean distances between the neighborhood points and anchors to examine whether one point can be selected for the feature extraction of anchors. The radius R , considering the timestamps of different frames, increases gradually with the time frame interval. A formula is used to calculate the radius:

$$R(a_i^j, p_i') = \tau \rho\left(\left\|t_i^j - t_i'\right\|\right), \quad (5)$$

where a_i^j and p_i' represents an anchor and an actual point around the anchor. t_i^j and t_i' are the timestamp of the anchor and the point separately. ρ represents a monotonically increasing function with increasing time intervals, and the increasing extent is controlled by a hyperparameter τ . $\|\cdot\|$ represents the absolute value of timestamp difference. Only the neighborhood

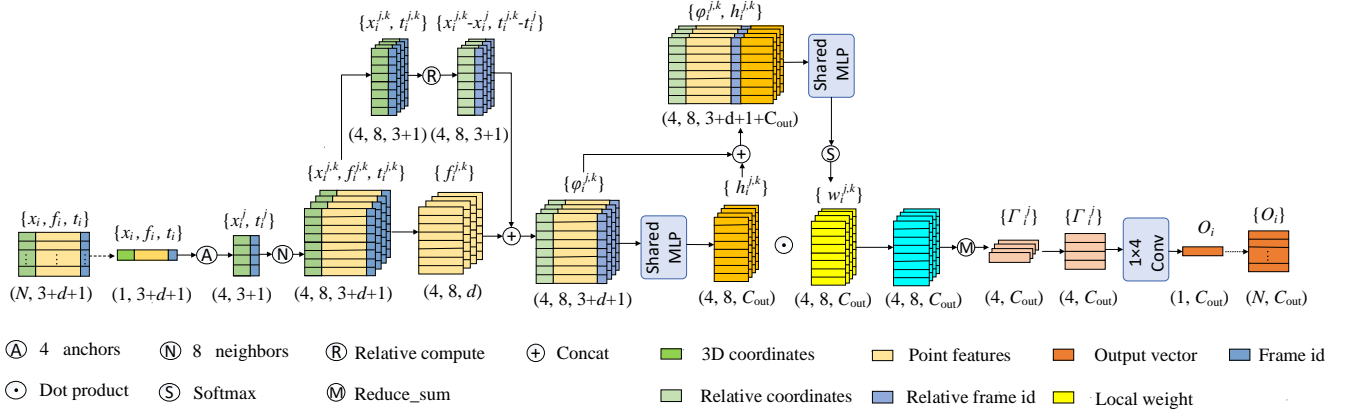


Figure 4. The detailed diagram of our anchor-based spatial-temporal attention convolution model. The input: N convolutional central core points. For the classification network and the encoding part of segmentation network, the core points are from Farthest Point Sampling (FPS). For the decoding part of segmentation network, the core points are propagated from the related encoding part, which is a common approach for upsampling in segmentation network of 3D point clouds [4]. The output: extracted features of the convolutional central core points.

points with distance from the anchors smaller than the related radius can be selected for the feature extraction.

Through this method, 8 neighborhood points from multiple frames $N_i^j = \{n_i^{j,k} = \{x_i^{j,k}, f_i^{j,k}, t_i^{j,k}\} | k = 1, 2, \dots, 8\}$ around an anchor a_i^j is selected for feature extraction. $x_i^{j,k}, f_i^{j,k}$ and $t_i^{j,k}$ represent the coordinates, raw features and timestamps of the selected points respectively.

2) *Relative Position, Relative Time, and Feature Encoding*: Around the core p_i , there are 4 anchors: $A_i = \{a_i^1, a_i^2, a_i^3, a_i^4\}$. Each anchor a_i^j chooses 8 neighborhood points $\{n_i^{j,1}, n_i^{j,2}, \dots, n_i^{j,8}\}$ from multiple frames. The relative spatial coordinates and timestamps of points are used to realize Euclidean space features and time features encoding respectively.

$$\varphi_i^{j,k} = ((x_i^{j,k} - x_i^j) \oplus \left\| t_i^{j,k} - t_i^j \right\| \oplus f_i^{j,k}), \quad (6)$$

where x_i^j and t_i^j represent the coordinates and timestamp of the anchor a_i^j . $x_i^{j,k}, t_i^{j,k}$ and $f_i^{j,k}$ represent the coordinates, timestamps, and raw features of the neighborhood points selected by this anchor. The feature $\varphi_i^{j,k}$ is used to obtain the features of anchor a_i^j before the embedding based on attention:

$$h_i^{j,k} = MLP(\varphi_i^{j,k}), \quad (7)$$

where $h_i^{j,k} \in \mathbb{R}^e$. The relative space and time information together with the raw features of the neighborhood points are input to a shared MLP for multimodal information fusion and encoding. Moreover, the relative spatial structure information and time information not only helps to determine the similarity of points but also influence the weight for the weighted attentive embedding later.

3) *Weighted attentive embedding*: In order to aggregate the encoded information $h_i^{j,k}$ of 8 neighborhood points without losing information, we give up the max pooling used in [2] and [4]. We expect to make use of these information in an adaptive weighted method. The gathered feature $\varphi_i^{j,k}$ introduced in equation (6) helps to decide the aggregation weights of the queried points:

$$w_i^{j,k} = softmax(MLP(\varphi_i^{j,k} \oplus h_i^{j,k})), \quad (8)$$

where $w_i^{j,k} \in \mathbb{R}^e$ and softmax activation function is used to normalize the attention. The embedding feature located at the anchor a_i^j is:

$$\Gamma_i^j = \sum_{k=1}^8 h_i^{j,k} \odot w_i^{j,k}, \quad (9)$$

where \odot means dot product. The proposed attentive method helps to distribute attention for all the neighborhood points around anchors reasonably, which improves the accuracy of the embedding features Γ_i^j aggregated from multiple frames. Then the features Γ_i^j ($j = 1, 2, 3, 4$) are convoluted to obtain the feature of central core point in Section III-A.

By this multi-frame fusion process, the receptive field of the central core point extends to the time dimension. The most significant difference between dynamic 3D point cloud sequences and a single-frame point cloud is that the inter-frame information in the point cloud sequences makes an enormous contribution to verifying the classification and segmentation results of each other.

As sometimes there may be no points in the local region around an anchor. A trick by setting zero is proposed to solve this problem. When an anchor can not found any points around, the feature value of this anchor is set to zero. In this training step, the trainable convolution weight will have no gradient update in this local feature extraction process. But the trainable convolution weight can be optimized in other regions in this step and be optimized in other training steps.

C. The Anchor-Based Spatial-Temporal Attention Convolutional Networks

In this section, we introduce two networks based on our ASTAConv model in detail. These two networks are designed respectively for classification and segmentation tasks from dynamic 3D point cloud sequences, shown in Fig. 5.

1) *The Network for Classification Task*: This network mainly consists of 3 Farthest Point Sampling (FPS) and ASTAConv operation with different sizes of MLPs. The initial input of this network is 3D point clouds from multiple

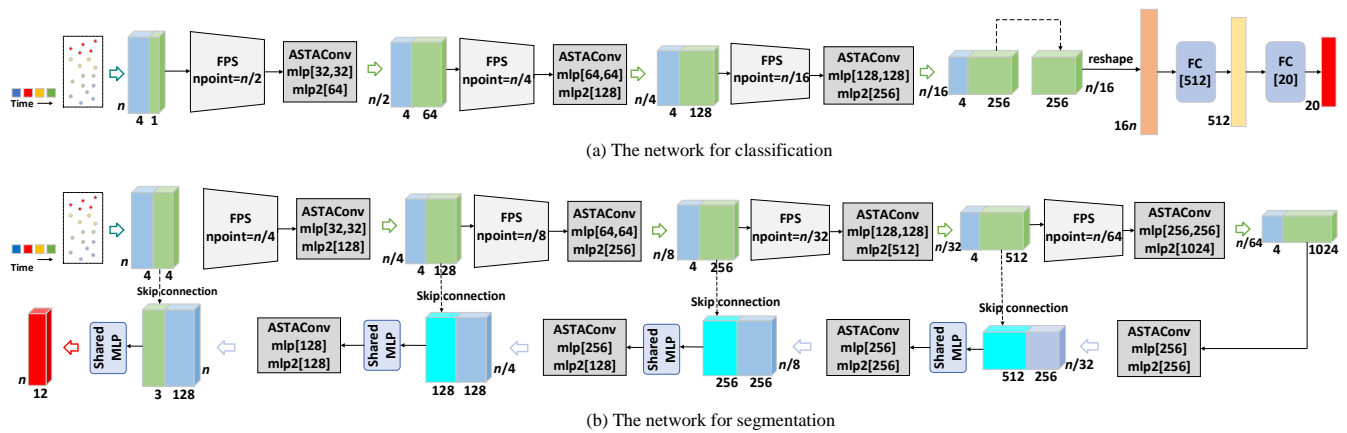


Figure 5. The detailed diagram of our anchor-based spatial-temporal attention convolutional network.

frames. The FPS acts as a point downsampling module for central core point selection. Then, 3D points are encoded by the ASTAConv. The structural features are extracted into sampled core points through the ASTAConv model. The final extracted features are fed into 2 Fully Connected (FC) layers, and the output is the classification results. The n of input dimension $n \times (4 + 1)$ presents the total number of points from multiple frames. The 4 presents 3D XYZ coordinates and 1D timestamp. The 1 presents the 1D timestamp. Because there are 20 classification classes for the action recognition on MSRA3D dataset [17] in Section IV-B, the output of classification network is 20D vector to present the class scores of 20 classes.

2) *Network for Segmentation Task*: The network of segmentation task has an encoder-decoder architecture like U-Net [32]. The encoding part of this network is similar to that of the classification network. The difference comes from the number of ASTAConv model and the channels of the Shared MLP. After 4 FPS layers and ASTAConv models, the output features are fed into the decoding part. During the decoding process, the output of the ASTAConv model is concatenated with the encoded features from skip connections, and then the combined features are fed into a Shared MLP. After 4 ASTAConv models and shared MLPs, the final output provides the results of the semantic segmentation for all the input points. The n of input dimension $n \times (4 + 4)$ presents the total number of points from multiple frames. The 4 presents 3D XYZ coordinates and 1D timestamp. The 1 presents 3D RGB color and 1D timestamp. Because there are 12 segmentation classes for the semantic segmentation on Synthia dataset [18] in Section IV-C, the output dimension of segmentation network is $n \times 12$ to present the segmentation scores of 12 classes for each point. Our classification and segmentation networks have the same input and output as MeteorNet [4] because we test on the same datasets.

IV. EXPERIMENTS AND EVALUATION

We designed the anchor-based spatial-temporal attention convolutional neural networks to learn the features from 3D point cloud sequences. Our networks not only learn from

 Table I
 CLASSIFICATION ACCURACY ON MSRACTION3D(%)

Input	Number of Frames	Method	Accuracy
Depth	20	Vieira et al. [33]	78.20
	18	Klase et al. [34]	81.43
Groundtruth skeleton	full	Actionlet [35]	88.21
Points	1	PointNet++ [2]	61.61
		Ours w/o attention	63.64
	4	MeteorNet [4]	78.11
		Ours	80.13
	8	MeteorNet [4]	81.14
		Ours	87.54
12	MeteorNet [4]	86.53	
	Ours	89.90	
16	MeteorNet [4]	88.21	
	Ours	91.24	
24	MeteorNet [4]	88.50	
	Ours	93.03	

multiple frames in an adaptive weighted method but also successfully extract the structural information. In this section, we will first describe the implementation details of our proposed models. Then our model is compared with the state-of-the-art models to show the superiority of our model. This is demonstrated in two tasks, action recognition and semantic segmentation. At last, several ablation studies are executed to analyze the contributions of our model.

A. Implementation

For action recognition, the initial learning rate is set as 0.001. For semantic segmentation, the initial learning rate is set as 0.0016. For both of them, the learning rate decreases by 0.7 every 200000 steps. The number of input points is the sum of the points from multiple frames. For action classification and semantic segmentation, the number of points in a single frame is respectively 2048 and 8192. The radii for querying neighborhood points for anchors are not only related to the timestamps of the points but also related to the density of point clouds in the current feature extraction level. After each FPS, we will double the radius to get a fixed number of neighborhood points in the sparser point clouds. For action

Table II
SEMANTIC SEGMENTATION RESULTS ON THE SYNTHIS DATASET

Number of Frames	Method	Blding	Road	Sdwlk	Fence	Vegitn	Pole	Car	T.sign	Pdstr	Bicyc	Lane	T.light	mIoU
1	4D MinkNet14 [15]	89.39	97.68	69.43	86.52	98.11	97.26	93.50	79.45	92.27	0.00	44.61	66.69	76.24
	PointNet++ [2]	96.88	97.72	86.20	92.75	97.12	97.09	90.85	66.87	78.64	0.00	72.93	75.17	79.35
	Ours w/o attention	98.35	98.72	93.28	96.56	98.84	97.91	95.35	75.36	82.81	0.00	77.05	80.78	82.92
2	MeteorNet [4]	97.65	97.83	90.03	94.06	97.41	97.79	94.15	82.01	79.14	0.00	72.59	77.92	81.72
	Ours	98.52	98.80	94.46	96.80	99.06	98.46	96.31	81.04	88.23	0.00	77.68	81.72	84.26
3	4D MinkNet14 [15]	90.13	98.26	73.47	87.19	99.10	97.50	94.01	79.04	92.62	0.00	50.01	68.14	77.46
	MeteorNet [4]	98.10	97.72	88.65	94.00	97.98	97.65	93.83	84.07	80.90	0.00	71.14	77.60	81.80
	Ours	98.59	98.83	94.77	97.16	99.25	98.60	96.39	83.24	88.21	0.00	78.13	82.27	84.62

classification, the initial radii for different frames are evenly distributed between 0.5 and 0.6 according to the timestamps, and for semantic segmentation, the radii are between 0.98 and 1.0, which is the same as [4]. Furthermore, the smallest radius is set to be equal to the distance between an anchor and its related central core point. BatchNorm [36] is used following each ASTAConv operation, and Adam optimizer [37] is adopted. Our method consumes the dynamic 3D point cloud sequences. Therefore, MSRAction3D dataset [17] and Synthia dataset [18] are preprocessed to generate dynamic 3D point cloud sequences as input for training and testing. All experiments are performed on a single RTX 2080Ti GPU.

B. Action Recognition

The proposed classification network is applied to action recognition on the MSRAction3D dataset [17]. This dataset contains 567 Kinect depth map sequences from 10 people with 20 actions: *high arm wave, horizontal arm wave, hammer, hand catch, forward punch, high throw, draw x, draw tick, draw circle, hand clap, two hand wave, side-boxing, bend, forward kick, side kick, jogging, tennis swing, tennis serve, golf swing, pick up & throw*. The dynamic 3D point cloud sequences are reconstructed by these depth map sequences. Some action examples are shown in Fig. 6. The training set and test set division is the same as the previous works [4], [35].

The classification results are shown in Table I. The evaluation metric is the average classification accuracy on the test set. We compare our method with the depth based methods [33], [34], ground truth skeleton based method [35], and the point cloud learning based methods [2], [4]. Note that PointNet++ [2] is a single point cloud learning method, while MeteorNet [4] is the leading method that consumes point cloud sequences, like ours. Therefore, the comparison between ours and MeteorNet [4] is fair. As shown in Table I, the result of ours with 12-frame input has even exceeded the 24-frame results of MeteorNet [4]. Finally, with 24-frame input, our method realizes more than 4% improvement over MeteorNet [4] and achieves new state-of-the-art.

The existence of anchors helps to dig out the hidden structural information from the point cloud sequences. Thereby, a more structural and comprehensive understanding of the sequential action improved the experimental results.

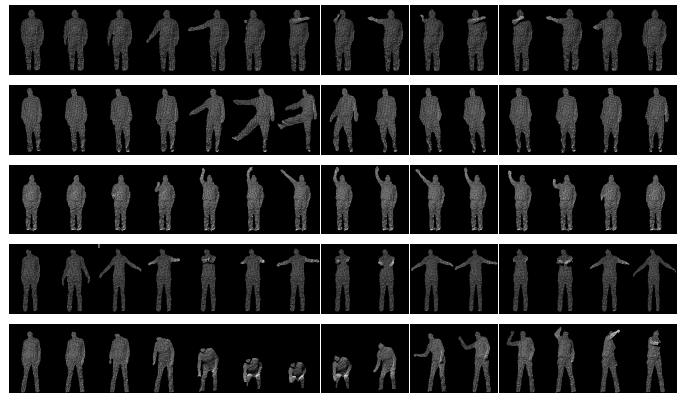


Figure 6. Some samples of MSRAction3D dataset [17]. From the top to the bottom: horizontal arm wave, side kick, high arm wave, hand clap, pickup & throw.

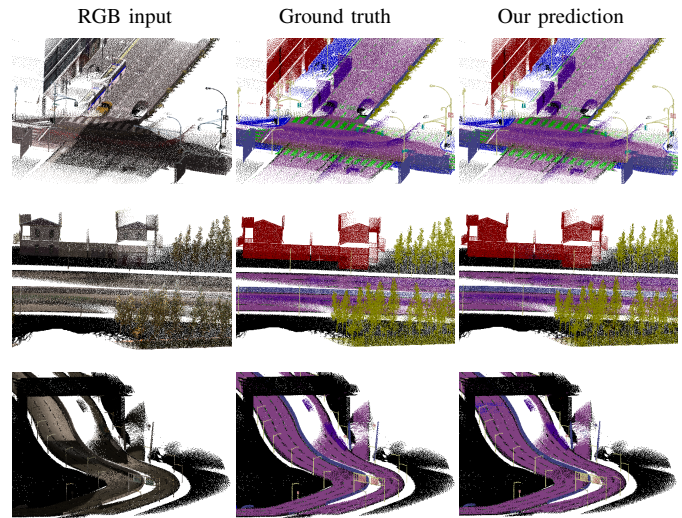


Figure 7. Visualized results on Synthia dataset [18]. Our method has a fine prediction in many details, such as street lamps, roads, and houses.

C. Semantic Segmentation

Our network for semantic segmentation is tested on the Synthia dataset [18]. Synthia dataset [18] is about driving scenarios and is used for semantic segmentation and related scene understanding tasks. The original video sequences are stereo RGBD images generated by 4 cameras located on the top of a moving car. In our task, RGB images and depth

Table III
ABLATION STUDIES OF SEMANTIC SEGMENTATION(%)

Number of Frames	Method	Blding	Road	Sdwlk	Fence	Vegitm	Pole	Car	T.sign	Pdstr	Bicyc	Lane	T.light	mIoU
2	MeteorNet [4]	97.65	97.83	90.03	94.06	97.41	97.79	94.15	82.01	79.14	0.00	72.59	77.92	81.72
	Ours w/o attention	98.37	98.79	94.26	96.56	98.98	98.12	95.88	78.96	87.66	0.00	77.70	81.86	83.93
	Ours (full, with attention)	98.52	98.80	94.46	96.80	99.06	98.46	96.31	81.04	88.23	0.00	77.68	81.72	84.26
3	MeteorNet [4]	98.10	97.72	88.65	94.00	97.98	97.65	93.83	84.07	80.90	0.00	71.14	77.60	81.80
	Ours w/o attention	98.39	98.80	94.50	96.96	99.08	98.45	96.04	84.82	85.17	0.00	78.03	81.54	84.31
	Ours (full, with attention)	98.59	98.83	94.77	97.16	99.25	98.60	96.39	83.24	88.21	0.00	78.13	82.27	84.62

Table IV
ABLATION STUDIES OF ACTION RECOGNITION. CLASSIFICATION ACCURACY IS USED FOR THE EVALUATION.(%)

Number of Frames	MeteorNet [4]	Ours w/o attention	Ours (full)
4	78.11	78.45	80.13
8	81.14	86.20	87.54
12	86.53	89.23	89.90
16	88.21	90.91	91.25
24	88.50	91.29	93.03

maps are utilized to generate the point cloud sequences. Overall, 6 video sequences in 9 different weather environments are preprocessed to create dynamic 3D point cloud sequences, which are used in our experiments. For each frame of dynamic point cloud sequences, a cube with a limit of $50m \times 50m \times 50m$ is built, where the moving car is in the center. Inside each frame, the FPS is applied to obtain 8192 points. The train/validation/test split is set as follows: Sequences 1-4 except for spring, sunset, and fog conditions are set as the training set. Sequence 5 is used as the validation set. Sunset and spring scenes in sequence 6 are used as the test set. Among the input dynamic 3D point cloud sequences, there are 19888 frames for the training set, 815 frames for the validation set, and 1,886 frames for the test set.

The results are listed in Table II. The evaluation metrics are based on per-class and mean Intersection-over-Union (IoU). Our method is compared with 4D MinkNet14 [15], PointNet++ [2] and recent work MeteorNet [4]. The model is tested by changing the number of input frames. Among the baselines, MeteorNet [4] is a method that performs semantic segmentation on raw 3D point cloud sequences, which is most similar to our method. Our method has better performance in most semantic classes and has the best results for the mIoU with different numbers of input frames. Compared with MeteorNet [4], ours has a little lower segmentation effect in the traffic sign class because the traffic sign is small and its structure is not obvious.

Some visualized results are presented in Fig. 7. It can be found that the proposed method achieves accurate semantic prediction for most points.

D. Ablation Study

The ablation studies are executed to further demonstrate the proposed contributions in this paper. The experiment settings are same with Section IV-B and Section IV-C except for ablation components.

1) *Anchor-Based 3D Convolution*: One of the most important components of our model is the anchor-based feature extraction. Through the anchors, central core points are able to excavate features in two steps with a structural method. To show the effect of anchors, we compare the result of ours without the attention encoding and that of MeteorNet [4] on action recognition task in Table IV. We find that the anchors help to improve the accuracy at least 2.5% for all the number of input frames except 4. For 4 frame input, the accuracy of our model only with anchors (w/o attention) also exceeds the MeteorNet [4] with a smaller part. There is an explanation for this. Most actions require a longer period to be confirmed and classified. For the input with a fewer number of frames, it is hard to get a significant improvement in accuracy even though we apply the anchor-based method. For the semantic segmentation, structure information for semantic awareness also exists in a single frame. Therefore, as shown in Table III, the performance gain also significant for fewer frame input by using the anchor-based method.

What's more, MeteorNet [4] will degenerate into PointNet++ [2] if the input changes to a single frame, while for our method, the anchor-based convolution can also be used for the input of a single frame. It is wondered if our anchor-based method benefits single frame input. We also test our anchor-based convolution on a single frame and compared it with PointNet++ [2] in Table I and Table II. Due to the difference between anchor-based convolution and shared MLP [2], ours obtains better performance than PointNet++ [2]. The results show the superiority of structured feature learning.

2) *Spatial-Temporal Attention Embedding*: Introduced in Section III-B, a weighted attentive embedding method is proposed during the feature gathering for the anchors. To demonstrate the effectiveness of this proposed method, we evaluate the networks with and without the attention both in action recognition and semantic segmentation. The experiment results of the two tasks are respectively shown in Table IV and Table III. The attention method improves the accuracy of both tasks for various input number of frames. With the spatial-temporal attention embedding, features are gathered in an adaptive weighted method, which distributes attention on the spatial-temporal information and focuses on beneficial area and time.

V. CONCLUSION

In this paper, a novel anchor-based spatial-temporal attention convolution operation (ASTACnv) and two networks

based on ASTAConv are proposed to directly consume dynamic 3D point cloud sequences. The anchor-based convolution naturally uses the 3D feature extraction approach and aggregates structured information from unstructured point clouds. To adaptively fuse the spatial-temporal information from point cloud sequences, spatial-temporal attention embedding is proposed and applied in the feature generation of anchors. Experiments on action recognition and semantic segmentation demonstrated the state-of-the-art performance of the proposed approach. The proposed convolution neural networks are expected to promote research and applications in the RGBD camera and LiDAR perception fields.

REFERENCES

- [1] C. R. Qi, H. Su, K. Mo, and L. J. Guibas, "Pointnet: Deep learning on point sets for 3d classification and segmentation," in *Proc. IEEE Conf. Comput. Vis. Pattern Recognit.*, 2017, pp. 652–660.
- [2] C. R. Qi, L. Yi, H. Su, and L. J. Guibas, "Pointnet++: Deep hierarchical feature learning on point sets in a metric space," in *Proc. Adv. Neural Inf. Process. Syst.*, 2017, pp. 5099–5108.
- [3] H. Thomas, C. R. Qi, J.-E. Deschard, B. Marcotegui, F. Goulette, and L. J. Guibas, "Kpconv: Flexible and deformable convolution for point clouds," in *Proc. IEEE Int. Conf. Comput. Vis.*, 2019, pp. 6411–6420.
- [4] X. Liu, M. Yan, and J. Bohg, "Meteornet: Deep learning on dynamic 3d point cloud sequences," in *Proc. IEEE Int. Conf. Comput. Vis.*, 2019, pp. 9246–9255.
- [5] P.-S. Wang, Y. Liu, Y.-X. Guo, C.-Y. Sun, and X. Tong, "O-cnn: Octree-based convolutional neural networks for 3d shape analysis," *ACM Trans. Graph.*, vol. 36, no. 4, pp. 1–11, 2017.
- [6] G. Riegler, A. Osman Ulusoy, and A. Geiger, "Octnet: Learning deep 3d representations at high resolutions," in *Proc. IEEE Conf. Comput. Vis. Pattern Recognit.*, 2017, pp. 3577–3586.
- [7] B. Graham, M. Engelcke, and L. van der Maaten, "3d semantic segmentation with submanifold sparse convolutional networks," in *Proc. IEEE Conf. Comput. Vis. Pattern Recognit.*, 2018, pp. 9224–9232.
- [8] Y. Ben-Shabat, M. Lindenbaum, and A. Fischer, "3dmfv: Three-dimensional point cloud classification in real-time using convolutional neural networks," *IEEE Robot. Autom. Lett.*, vol. 3, no. 4, pp. 3145–3152, 2018.
- [9] Z. Kuang, J. Yu, S. Zhu, Z. Li, and J. Fan, "Effective 3-d shape retrieval by integrating traditional descriptors and pointwise convolution," *IEEE Transactions on Multimedia*, vol. 21, no. 12, pp. 3164–3177, 2019.
- [10] D. Wang, H. Yao, F. Tombari, S. Zhao, B. Wang, and H. Liu, "Learning descriptors with cube loss for view-based 3-d object retrieval," *IEEE Transactions on Multimedia*, vol. 21, no. 8, pp. 2071–2082, 2019.
- [11] C. Xu, B. Leng, B. Chen, C. Zhang, and X. Zhou, "Learning discriminative and generative shape embeddings for 3d shape retrieval," *IEEE Transactions on Multimedia*, 2019.
- [12] J. Mao, X. Wang, and H. Li, "Interpolated convolutional networks for 3d point cloud understanding," in *Proc. IEEE Int. Conf. Comput. Vis.*, 2019, pp. 1578–1587.
- [13] Q. Hu, B. Yang, L. Xie, S. Rosa, Y. Guo, Z. Wang, N. Trigoni, and A. Markham, "Randla-net: Efficient semantic segmentation of large-scale point clouds," *arXiv preprint arXiv:1911.11236*, 2019.
- [14] G. Wang, Y. Yang, H. Zhang, Z. Liu, and H. Wang, "Spherical interpolated convolutional network with distance-feature density for 3d semantic segmentation of point clouds," 2020.
- [15] C. Choy, J. Gwak, and S. Savarese, "4d spatio-temporal convnets: Minkowski convolutional neural networks," in *Proc. IEEE Conf. Comput. Vis. Pattern Recognit.*, 2019, pp. 3075–3084.
- [16] W. Luo, B. Yang, and R. Urtasun, "Fast and furious: Real time end-to-end 3d detection, tracking and motion forecasting with a single convolutional net," in *Proc. IEEE Conf. Comput. Vis. Pattern Recognit.*, 2018, pp. 3569–3577.
- [17] W. Li, Z. Zhang, and Z. Liu, "Action recognition based on a bag of 3d points," in *Proc. IEEE Int. Conf. Comput. Vis. Pattern Recognit. Workshops (CVPRW)*. IEEE, 2010, pp. 9–14.
- [18] G. Ros, L. Sellart, J. Materzynska, D. Vazquez, and A. M. Lopez, "The synthia dataset: A large collection of synthetic images for semantic segmentation of urban scenes," in *Proc. IEEE Conf. Comput. Vis. Pattern Recognit.*, 2016, pp. 3234–3243.
- [19] H. Su, V. Jampani, D. Sun, S. Maji, E. Kalogerakis, M.-H. Yang, and J. Kautz, "Splatnet: Sparse lattice networks for point cloud processing," in *Proc. IEEE Conf. Comput. Vis. Pattern Recognit.*, 2018, pp. 2530–2539.
- [20] Y. Xu, T. Fan, M. Xu, L. Zeng, and Y. Qiao, "Spidernn: Deep learning on point sets with parameterized convolutional filters," in *Proc. Eur. Conf. Comput. Vis. (ECCV)*, 2018, pp. 87–102.
- [21] A. Komarichev, Z. Zhong, and J. Hua, "A-cnn: Annularly convolutional neural networks on point clouds," in *Proc. IEEE Conf. Comput. Vis. Pattern Recognit.*, 2019, pp. 7421–7430.
- [22] H. Lei, N. Akhtar, and A. Mian, "Octree guided cnn with spherical kernels for 3d point clouds," in *Proc. IEEE Conf. Comput. Vis. Pattern Recognit.*, 2019, pp. 9631–9640.
- [23] H. Zhao, L. Jiang, C.-W. Fu, and J. Jia, "Pointweb: Enhancing local neighborhood features for point cloud processing," in *Proc. IEEE Conf. Comput. Vis. Pattern Recognit.*, 2019, pp. 5565–5573.
- [24] Y. Wang, Y. Sun, Z. Liu, S. E. Sarma, M. M. Bronstein, and J. M. Solomon, "Dynamic graph cnn for learning on point clouds," *ACM Trans. Graph.*, vol. 38, no. 5, pp. 1–12, 2019.
- [25] Z. Zhang, B.-S. Hua, and S.-K. Yeung, "Shellnet: Efficient point cloud convolutional neural networks using concentric shells statistics," in *Proc. IEEE Int. Conf. Comput. Vis.*, 2019, pp. 1607–1616.
- [26] W. Wu, Z. Y. Wang, Z. Li, W. Liu, and L. Fuxin, "Pointpwc-net: Cost volume on point clouds for (self-) supervised scene flow estimation," in *European Conference on Computer Vision*. Springer, 2020, pp. 88–107.
- [27] G. Wang, X. Wu, Z. Liu, and H. Wang, "Hierarchical attention learning of scene flow in 3d point clouds," *arXiv preprint arXiv:2010.05762*, 2020.
- [28] X. Gu, Y. Wang, C. Wu, Y. J. Lee, and P. Wang, "Hplflownet: Hierarchical permutohedral lattice flownet for scene flow estimation on large-scale point clouds," in *Proc. IEEE Conf. Comput. Vis. Pattern Recognit.*, 2019, pp. 3254–3263.
- [29] M. Kiefel, V. Jampani, and P. Gehler, "Permutohedral lattice cnns," in *ICLR Workshop Track 2015*, 2015.
- [30] V. Jampani, M. Kiefel, and P. V. Gehler, "Learning sparse high dimensional filters: Image filtering, dense crfs and bilateral neural networks," in *Proceedings of the IEEE Conference on Computer Vision and Pattern Recognition*, 2016, pp. 4452–4461.
- [31] X. Liu, C. R. Qi, and L. J. Guibas, "Flownet3d: Learning scene flow in 3d point clouds," in *Proc. IEEE Conf. Comput. Vis. Pattern Recognit.*, 2019, pp. 529–537.
- [32] O. Ronneberger, P. Fischer, and T. Brox, "U-net: Convolutional networks for biomedical image segmentation," in *International Conference on Medical image computing and computer-assisted intervention*. Springer, 2015, pp. 234–241.
- [33] A. W. Vieira, E. R. Nascimento, G. L. Oliveira, Z. Liu, and M. F. Campos, "Stop: Space-time occupancy patterns for 3d action recognition from depth map sequences," in *Progress in Pattern Recognition, Image Analysis, Computer Vision, and Applications (CIARP)*. Springer, 2012, pp. 252–259.
- [34] A. Klaser, M. Marszałek, and C. Schmid, "A spatio-temporal descriptor based on 3d-gradients," in *Proc. Brit. Mach. Vis. Conf.*, 2008, pp. 275:1–10.
- [35] J. Wang, Z. Liu, Y. Wu, and J. Yuan, "Mining actionlet ensemble for action recognition with depth cameras," in *Proc. IEEE Conf. Comput. Vis. Pattern Recognit.* IEEE, 2012, pp. 1290–1297.
- [36] S. Ioffe and C. Szegedy, "Batch normalization: Accelerating deep network training by reducing internal covariate shift," *arXiv preprint arXiv:1502.03167*, 2015.
- [37] D. P. Kingma and J. Ba, "Adam: A method for stochastic optimization," *arXiv preprint arXiv:1412.6980*, 2014.



Guangming Wang received the B.S. degree from Department of Automation from Central South University, Changsha, China, in 2018. He is currently pursuing the Ph.D. degree in Control Science and Engineering with Shanghai Jiao Tong University. His current research interests include SLAM and computer vision, in particular, deep learning on point clouds.



Hanwen Liu is currently pursuing the B.Eng. degree in Department of Computer Science and Engineering, Shanghai Jiao Tong University. His latest research interests include 3D point clouds and computer vision



Hesheng Wang (SM'15) received the B.Eng. degree in electrical engineering from the Harbin Institute of Technology, Harbin, China, in 2002, and the M.Phil. and Ph.D. degrees in automation and computer-aided engineering from The Chinese University of Hong Kong, Hong Kong, in 2004 and 2007, respectively. He was a Post-Doctoral Fellow and Research Assistant with the Department of Mechanical and Automation Engineering, The Chinese University of Hong Kong, from 2007 to 2009. He is currently a Professor with the Department of Automation, Shanghai Jiao Tong University, Shanghai, China. His current research interests include visual servoing, service robot, adaptive robot control, and autonomous driving. Dr. Wang is an Associate Editor of Assembly Automation and the International Journal of Humanoid Robotics, a Technical Editor of the IEEE/ASME TRANSACTIONS ON MECHATRONICS. He served as an Associate Editor of the IEEE TRANSACTIONS ON ROBOTICS from 2015 to 2019. He was the General Chair of the IEEE RCAR 2016, and the Program Chair of the IEEE ROBIO 2014 and IEEE/ASME AIM 2019.



Muyao Chen is currently pursuing the B.S. degree in Department of Computer Science and Engineering, Shanghai Jiao Tong University. His latest research interests include 3D point clouds and computer vision.



Yehui Yang is currently pursuing the B.S. degree in Department of Automation, Shanghai Jiao Tong University. His latest research interests include SLAM and computer vision.



Zhe Liu received his B.S. degree in Automation from Tianjin University, Tianjin, China, in 2010, and Ph.D. degree in Control Technology and Control Engineering from Shanghai Jiao Tong University, Shanghai, China, in 2016. From 2017 to 2020, he was a Post-Doctoral Fellow with the Department of Mechanical and Automation Engineering, The Chinese University of Hong Kong, Hong Kong. He is currently a Research Associate with the Department of Computer Science and Technology, University of Cambridge. His research interests include

autonomous mobile robot, multirobot cooperation and autonomous driving system.